ILU-12 COMMISSIONING

V.L. Auslender, A.A. Bryazgin, K.N. Chernov, V.G. Cheskidov, B.L. Factorovich, V.A. Gorbunov, I.V. Gornakov, M.V. Korobejnikov, G.I. Kuznetsov, A.N. Lukin, I.G. Makarov, N.V. Matyash, G.N. Ostreiko, A.D. Panfilov, G.V. Serdobintsev, V.V. Tarnetsky, M.A. Tiunov, V.O. Tkachenko, A.A. Tuvik
Budker INP SB RAS, Novosibirsk, Russia
E-mail: M.A.Tiunov@inp.nsk.su; Phone: +7(383)339-45-54

At Budker INP SB RAS, a prototype of high-power industrial electron accelerator for the energy of 5 MeV, named ILU-12, has been successfully commissioned. The accelerator operates at 176 MHz. The paper presents the accelerator concept together with simulation results for the accelerating structure, beam injection and dynamics.

The obtained beam pulsed power of 1,5 MW at the structure electron efficiency of 67% is close to the simulation value. Improvements of beam transportation and energy spectrum due to the injection regime optimization were experimentally proven. The results obtained are discussed.

PACS: 29.17+w

1. INTRODUCTION

The work on creation of the prototype for industrial linear RF accelerator with electron energy of 5 MeV and average beam power up to 300 kW has been carrying out at Budker INP SB RAS since 2002 [1-4]. The work is supported by DoE as a part of ISTC Project #2550. The goals of the Project are development of the conception of low-price but reliable industrial accelerator with minimal maintenance cost, and also manufacturing of the accelerator prototype named ILU-12 together with all the equipment required for its final testing. During the tests, the prototype might reach electron energy of 5 MeV and beam pulsed power of 1,5…2 MW and also demonstrate the possibility of high-power industrial accelerator creation on its base.

Accelerator ILU-12 was assembled and successfully commissioned in early this year. The paper shortly describes the developed concept of high-power industrial accelerator and also presents the results of numerical simulation and measurements of the accelerator prototype main parts. The results of first experiments carried out at ILU-12 accelerator are described in details and compared with simulation results.

2. ACCELERATOR CONCEPT

Figure presents the developed block diagram of high-power industrial accelerator [3].

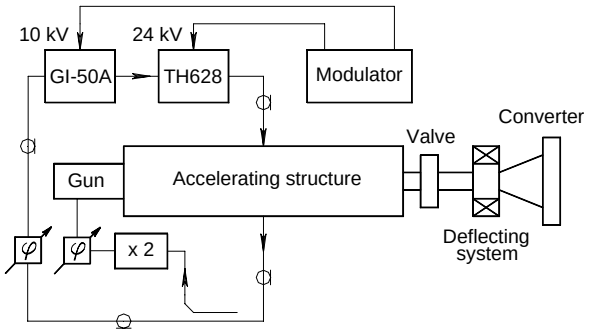

Fig.1. Accelerator block diagram

The main accelerator parts are: accelerating structure, vacuum tube two-stage amplifier, modulator, triode RF gun.

The first feature of the accelerator is the use of low-frequency multiple-cavity standing wave structure with on-axis coupling cells. The structure has increased efficiency as compared with a single-cavity accelerator because of reduced power losses per cavity at fixed average beam power. A generator based on vacuum tubes with efficiency up to 80%, for example on THALES (France) TH628 diacrode may be developed for the structure excitation.

The second feature of the accelerator is that the electron triode RF gun placed directly into the first accelerating gap is used as an electron source. An additional RF voltage is applied to the cathode-grid gap to provide a narrow energy spectrum of high-power electron beam, which is required for effective energy conversion into X-rays, and lossless transportation of the beam through the accelerating structure.

The third feature is the use of a two-stage generator with feedback circuit closed via the accelerating structure. So, there is no need in a frequency stabilization system for the accelerating structure or generator that simplifies the generator and accelerator control system.

The developed concept allowed us to considerably simplify the accelerator design and reduce its total cost as well as improve its reliability and reduce maintenance costs.

3. DESIGN, MANUFACTURING AND MEASUREMENTS OF ILU-12 COMPONENTS

3.1. ACCELERATING STRUCTURE

Fig.2 presents the general view of the ILU-12 accelerating structure which contains three whole and two half accelerating cells, and four coupling cells [2,3]. It is a biperiodical structure with on-axis coupling cavities, operating in standing wave mode at 176,3 MHz. Magnetic field coupling is provided by coupling slots. To prevent the coupling through the cell, the coupling slots in coupling cell opposite walls are rotated by 90° from one another. Operating mode is E_{010}.

Accelerating cavities were optimized with SuperLANS program [5] by quality factor and surface RF fields. Simulations show that structure efficiency higher

PROBLEMS OF ATOMIC SCIENCE AND TECHNOLOGY. 2008. № 3.
Series: Nuclear Physics Investigations (49), p.20-24.

than 70% for given electron energy of 5 MeV may be obtained with four whole accelerating cavities [3].

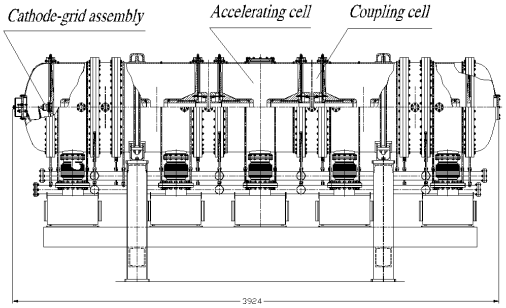

Fig.2. General view of the accelerating structure

The developed system for the structure accelerating cavities water cooling is presented in Fig.3. Simulations show that the major part (5 kW) of average RF power losses correspond to the outer surface of the accelerating cell coaxial electrode. The electrode has a separate water cooling branch made with copper pipe with the inner diameter of 8 мм. The pipe is laid inside the electrode near the outer surface. The cavity vertical wall has its own water cooling branch made with the same pipe. Power losses amount to 4 kW per wall surface. Power losses in the shell inner surface amount to 2.3 kW, the surface is cooled by two parallel brunches made as copper rectangular wires with inner aperture of Ø 8.5 diameter, soldered to the outer surface of the shell.

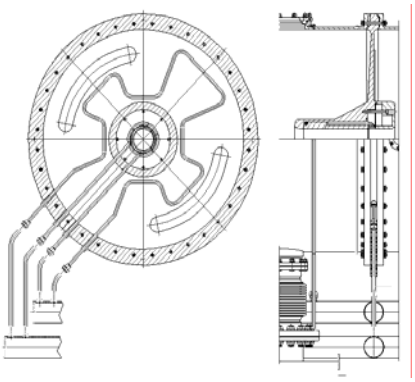

Fig.3. Water cooling of the disc and coaxial part

Accelerating structure cavity manufacturing was completed in December, 2006 года. In February, 2007, the accelerating structure was assembled upright without indium sealing for measurements and adjusting the cell partial frequencies.

The partial frequency of the accelerating structure cell may be measured if the eigen frequencies of the neighbor cells are detuned enough. The detuning was carried out with two copper rods introduced into the structure along the axis from the opposite sides; the detuning "quality" was verified by numerical simulation. The measured frequency spread of the accelerating cells did not exceed $\pm 10^{-3}$ due to high accuracy of manufacturing. Coupling cell frequencies were lower than the operating frequency by ~9 MHz, their adjustment was provided by turning the central replaceable cylinders. After frequency adjustments and surface cleaning, the structure was assembled with indium sealing for final measurements of the cell partial frequencies (Fig.4).

To find the accelerating structure stop-band, the frequencies of $\pi/2$ modes of two coupling cavity chains with different end cells were measured. The stop-band is 0.034 MHz that is a good result.

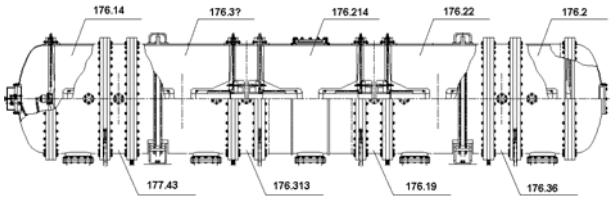

Fig.4. Partial frequencies of the cells after assembling with indium sealing

Experimental dispersion curve of ILU-12 accelerating structure is shown in Fig.5. It is in good agreement with 3D simulation results obtained with CST Microwave Studio [6] and symmetric enough relative to the $\pi/2$ mode, so the neighbor coupling frequencies are maximally distanced from the operating frequency.

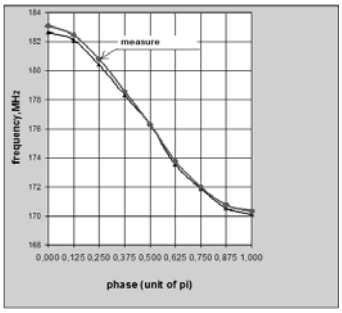

Fig.5. Simulated and measured dispersion curves of the accelerating structure

The bead-pull measurements were carried out to find the accelerating field amplitude distribution along the structure. The results are in good agreement with 3D simulation predictions.

Main measured parameters of the accelerating structure assembled with indium sealing are listed in Table.

Operating frequency, MHz	176.308
Quality factor	~21000
Characteristic impedance, Ω	824
Shunt impedance, MΩ	17.3

3.2. CATHODE-GRID UNIT

The cathode-grid unit [7], specially designed for ILU-12 accelerator, is shown in Fig.6.

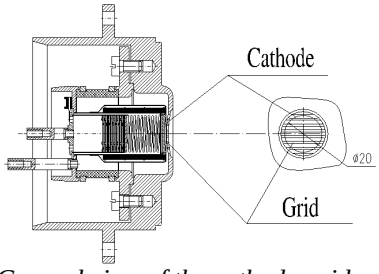

Fig.6. General view of the cathode-grid assembly

The main feature of the assembly is the use of a slot grid formed by equidistant parallel wires of different length. Such grid has higher transparency as compared to cellular grid and, moreover, its electron-optic characteristics may be simulated with high accuracy using 2D software [7,8].

A full-scale prototype of the cathode assembly with LaB_6 emitter of 20 mm diameter [4] was designed,

manufactured, and tested to verify the voltage-current characteristic stability of the electron gun for ILU-12 accelerator. The assembly longitudinal size is about two times shorter than that of the unit previously used in ILU-type accelerators.

Fig.7 presents simulated and measured grid potential dependence of the cathode average current for that assembly at extraction field of 60 kV/cm on the grid surface.

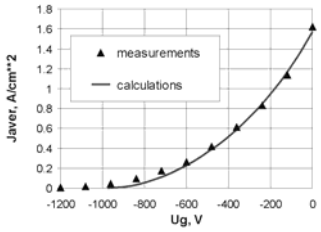

Fig.7. Experimental and calculated grid-cathode potential dependencies of average current density of the grid-cathode assembly for E_{acc}=60 kV/cm

3.3. BEAM INJECTION AND DYNAMICS SIMULATION

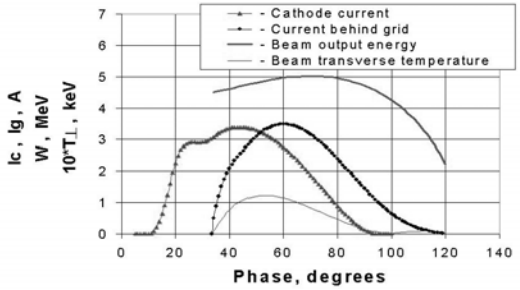

Fig.8. Accelerating field on the cathode phase dependencies of the current micro pulse and beam output parameters

Electric field phase in the first gap dependencies of the main electron beam initial and output parameters were simulated for ILU-12 accelerator in quasistationary 2D approximation with paying regards to transit time angles and beam space charge effects (Fig.8) [7].

It was proposed to apply an additional RF voltage of the operating frequency with proper amplitude and phase to the cathode-grid gap for the accelerating electron spectrum narrowing and longitudinal dynamics optimization. Figs.8-9 present result obtained at phase and amplitude optimized additional RF voltage. 3D model of the cathode-grid unit was developed on the base of 2D simulation results for beam initial parameters; electron trajectory analysis in the accelerating structure was carried out (Fig.9) [7].

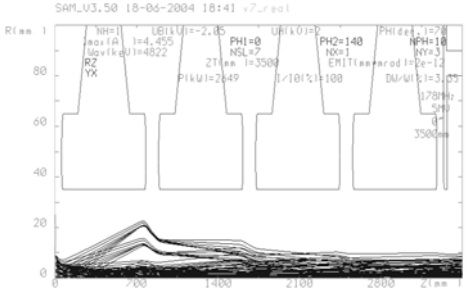

Fig.9. Typical electron trajectories in the accelerator

The simulations allowed us to choose the optimal structure period and aperture as well as radius of curvature for the cathode-grid unit sphere.

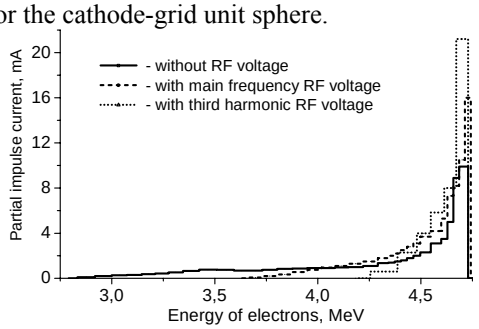

Fig.10. Measured electron beam energy spectrums at ILU-10 output

At ILU-10 machine, the possibility to narrow the electron spectrum by applying an additional RF voltage to the cathode-grid gap was experimentally proven (Fig.10) [9].

4. ILU-12 COMMISSIONING

4.1. RF CONDITIONING AND TESTS OF THE STRUCTURE AT FULL VOLTAGE

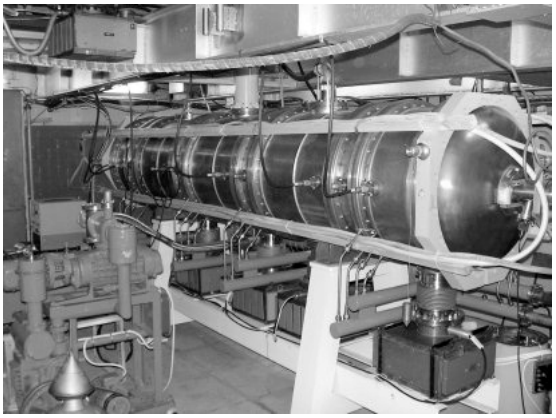

Fig.11. Accelerating structure after installation

After cold measurements the structure was vacuum-proof assembled and installed in horizontal (operating) position (Fig.11). Then, the ion pumps were connected. After 6-hour pumping, vacuum of $5 \cdot 10^{-6}$ Torr was obtained. It is a good result for a system with no previous heating.

After short-term conditioning, the multipactor was overcome. At pulse repetition rate of (1…25) Hz, 3 hour of conditioning was enough (good achievement!). The maximal accelerating voltage level of 7.5 MV was also achieved in several hours.

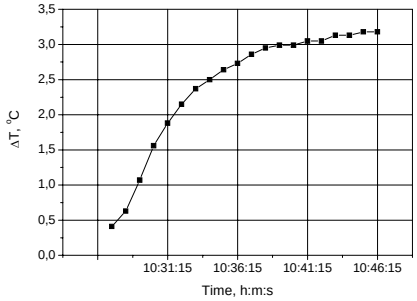

Fig.12. Measured time dependence of the temperature gradient in the accelerating cell coaxial part cooling system

The accelerating structure cooling system efficiency was experimentally verified in the actual industrial accelerator operating regime. To do so, the regime with 10 kW of average power was released in the structure, that was 10 times lower, that in the operating mode. The water flow was also decreased by a factor of 10 in relation to the operating mode and amounted to 30 l/min. The time dependence of the temperature gradient on the cooling system was measured for the accelerating cell coaxial part with maximal relative power losses (Fig.12). The steady temperature gradient was a little higher than 3°C.

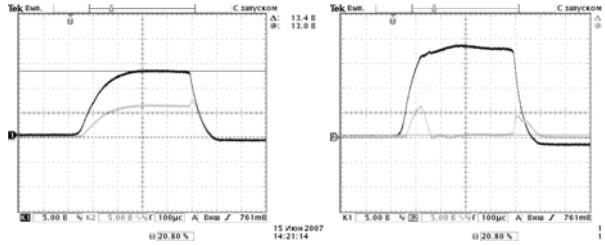

a) *b)*

Fig.13. Measurement results for amplitudes of incident (bold curves) and reflected (plane curves) waves without (a) and with (b) the electron beam in the structure

After that, the coupling between the accelerator and supplying feeder from the RF generator was optimized for operation with ~450…500 mA electron currents by turning the coupling loop. The measurement results for incident and reflected waves with no current in the structure are shown in Fig.13,a. One can see that reflected wave amplitude reaches half the incident wave amplitude (unmatched regime with reflection factor Γ=0.5). Fig.13,b presents the measurement results at the cathode beam current of 300 mA with an additional RF voltage applied to the gun cathode. Reflected wave amplitude is close to zero (matched mode).

4.2. ELECTRON BEAM TRANSPORTATION

To optimize beam transportation through the accelerating structure, measurements were carried out for the beam current from the cathode and at the structure output with the Faraday cup placed at 1150 mm distance from the accelerator output flange. Beam current passing was measured with and without applying an additional RF voltage of the main harmonic to the gun cathode. The specified beam current from the cathode was kept up with the feedback system.

The first experiments with no RF voltage on the cathode resulted in 50% current passing with strong vacuum chamber heating near the accelerating structure output. Beam displacement from the axis was effected by the geomagnetic field of about 1 Gs. To compensate that field, four Helmholtz coils with the length of 4.5 m and width of 0.8 m was installed along the whole structure (see Fig.11).

After installation of Helmholtz coils with optimal currents, the vacuum chamber heating was completely overcome along the full structure length. The electron beam passing through the structure was increased up to 80% with no RF voltage, and up to 96% with applying an additional RF voltage on the gun cathode. The results are in good agreement with beam injection and dynamics simulation results. Measurement results for beam cathode current of 300 mA passing with and without additional RF voltage with amplitude of 0.7 kV are shown in Fig.14.

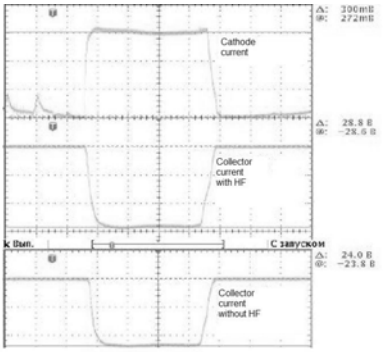

Fig.14. Oscillograms of the cathode current (top) and Faraday cup current with additional RF voltage on the cathode (middle) and with no additional RF voltage (bottom). Cathode current of 300 mA, collector current of 288 mA with RF voltage, 240 mA without RF voltage

Pulsed cathode current of 350 mA at 95% current passing was obtained by applying the phase and amplitude optimized RF voltage to the cathode-grid gap. The accelerated current was limited by the maximum pulsed power (~2,3MW) of the generator triode tube.

4.3. BEAM ENERGY SPECTRUM MEASUREMENTS

Accelerated electron energy was measured with magnetic spectrometer which was placed at the accelerator output and supplied with its own Faraday cup. Two collimating slots of 2 mm width were installed at the spectrometer input and output. The maximum of the spectral distribution was assumed to be the accelerated beam energy value.

Fig.15 presents the measured beam spectrums at the cathode current of 300 mA with and without additional RF voltage with amplitude of 0.7 kV. Evidently that maximal current at the spectrometer output increases with the additional RF voltage applying and shifts to higher energy area. According to simulations, the effect takes place due to injection of current micro pulses at earlier phases of the accelerating field.

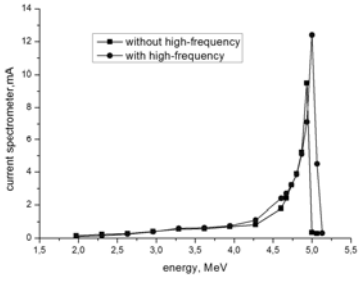

Fig.15. Dependence of current at the spectrometer output from energy of electrons

4.4. BEAM TRANSVERSE DIMENSIONS MEASUREMENTS

Measurements of the beam spot size at the accelerating structure output were carried out by burning the hole in 0.25 mm foil. The foil was placed before the Faraday cup at 1150 mm distance from the structure output; two

regimes were realized – with and without applying additional RF voltage on the triode gun cathode. Pulsed cathode current was 200 mA in both cases. Exposure time of the beam on the foil was about 2 minutes (time of reaching the steady-state Faraday cup current).

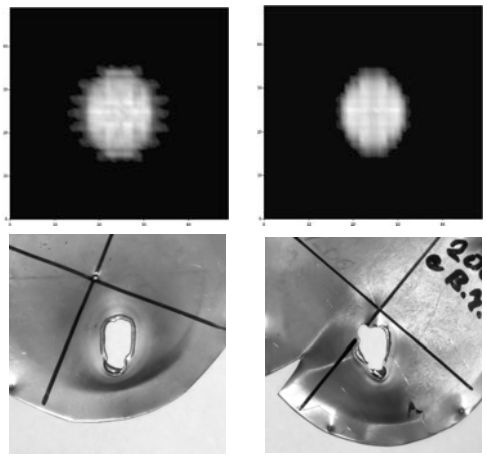

Fig.16. Simulated and experimental beam cross-section

Fig.16 presents simulated (top) and experimental (bottom) 200 mA beam cross-section for two beam transportation regimes: without (left) and with (right) the additional RF voltage on the triode RF gun cathode. The real size of pictures is 50×50 mm. There is a good agreement between simulation and experimental results except for the apparent beam halo in photos. The beam has the maximal size in direction orthogonal to the grid slots, as it was predicted by simulations.

SUMMARY

At Budker INP SB RAS, successful commissioning of ILU-12 accelerator was carried out. The following accelerator parameters were obtained:

- pulsed cathode current of 350 mA;
- beam current passing through the accelerating structure of 95%;
- vaximal electron energy at the accelerator output of 5 MeV;
- beam pulsed power of 1.5 MW;
- accelerating structure electron efficiency of 67%.

Possibility of a high-power industrial accelerator creation on the base of that prototype was experimentally shown. Beam average power of 300 kW at electron energy of 5 MeV may be obtained with the use of TH628 diacrode based RF generator.

The accelerator may operate at the energy up to 7.5 MeV, and electron beam power may exceed 300 kW by adding two more accelerating cells to the accelerating structure.

REFERENCES

1. V. Auslender, et al. Radiation Physics and Chemistry 63 2002, p.613-615.
2. M. Tiunov, et al. *Proceedings of EPAC 2002*. Paris, France, 2002, p.2813-2815.
3. V.L. Auslender, et al. // *Problems of Atomic Science and Technology. Series: "Nuclear Physics Investigations" (43).* 2004, №2, p.6-8.
4. V.L. Auslender, et al. *Proceedings of PAC 2005.* Knoxville, USA, 2005, p.1502-1504.
5. D. Myakishev, V. Yakovlev. *Proceedings of IEEE Part. Accel. Conf.* 1991, v.5, p.3002-3004.
6. http://www.cst.de
7. M.A. Tiunov, et al. *Proceedings of PAC 2005*. Knoxville, USA, 2005, p.1419-1421.
8. B.M. Fomel, et al. Preprint BINP 96-11, 1996.
9. V.L. Auslender, et al. *Proceedings of the RuPAC 2004.* Dubna, JINR, 2005, p.116-120.

ЗАПУСК УСКОРИТЕЛЯ ИЛУ-12

В.Л. Ауслендер, А.А. Брязгин, К.Н. Чернов, В.Г. Ческидов, Б.Л. Факторович, В.А. Горбунов, И.В. Горнаков, М.В. Коробейников, Г.И. Кузнецов, А.Н. Лукин, И.Г. Макаров, Н.В. Матяш, Г.Н. Острейко, А.Д. Панфилов, Г.В. Сердобинцев, В.В. Тарнецкий, М.А. Тиунов, В.О. Ткаченко, А.А. Тувик

В ИЯФ СО РАН произведен успешный запуск прототипа мощного промышленного ускорителя электронов ИЛУ-12 на энергию 5 МэВ. Рабочая частота ускорителя 176 МГц. В докладе кратко описывается концепция ускорителя. Приводятся результаты расчетов ускоряющей структуры, инжекции и динамики пучка.

Получены близкие к расчетным импульсная мощность пучка (1,5 МВт) и электронный КПД ускоряющей структуры (67%). Экспериментально подтверждено улучшение прохождения пучка и его энергетического спектра с помощью оптимизации режима инжекции. Обсуждаются полученные результаты.

ЗАПУСК ПРИСКОРЮВАЧА ІЛУ-12

В.Л. Ауслендер, А.А. Брязгін, К.Н. Чернов, В.Г. Ческідов, Б.Л. Факторович, В.А. Горбунов, І.В. Горнаков, М.В. Коробейников, Г.І. Кузнецов, А.Н. Лукін, І.Г. Макаров, Н.В. Матяш, Г.Н. Острейко, А.Д. Панфілов, Г.В. Сердобінцев, В.В. Тарнецький, М.А. Тіунов, В.О. Ткаченко, А.А. Тувік

В ІЯФ СВ РАН зроблено успішний запуск прототипу потужного промислового прискорювача електронів ІЛУ-12 на енергію 5 МеВ. Робоча частота прискорювача 176 МГц. Коротко описується концепція прискорювача. Приводяться результати розрахунків прискорювальної структури, інжекції і динаміки пучка.

Отримано близькі до розрахункових імпульсна потужність пучка (1,5 МВт) і електронний ККД прискорювальної структури (67%). Експериментально підтверджено поліпшення проходження пучка і його енергетичного спектра за допомогою оптимізації режиму інжекції. Обговорюються отримані результати.